Journal of Photochemistry and Photobiology A: Chemistry 227 (2012) 11–17

Contents lists available at SciVerse ScienceDirect

Journal of Photochemistry and Photobiology A: Chemistry

journal homepage: www.elsevier.com/locate/jphotochem

High power impulse magnetron sputtering (HIPIMS) and traditional pulsed sputtering (DCMSP) Ag-surfaces leading to *E. coli* inactivation

O. Baghriche[a], A.P. Ehiasarian[b], E. Kusiak-Nejman[a,c], C. Pulgarin[a,*], R. Sanjines[d], A.W. Morawski[c], J. Kiwi[e,*]

[a] Group of Electrochemical Engineering, EPFL-SB-ISIC-GGEC, Station 6, CH-1015 Lausanne, Switzerland
[b] Material and Engineering Research Institute Sheffield Hallam University, Howard St, Sheffield S1 1WB, UK
[c] West Pomerianian University of Technology, Szczecin, Institute of Chemical and Environment Engineering, Pulaskiego 10, 70-322 Szczecin, Poland
[d] EPFL-SB-IPMC-LNNME, Bât PH, Station 3, CH-1015 Lausanne, Switzerland
[e] Laboratory of Photonics and Interfaces, EPFL-SB-ISIC-LPI, Bât Chimie, Station 6, CH-1015 Lausanne, Switzerland

ARTICLE INFO

Article history:
Received 20 June 2011
Received in revised form 9 October 2011
Accepted 15 October 2011
Available online 29 October 2011

Keywords:
HIPIMS
DCMSP
Sputtering
Ag-nanoparticle films
E. coli
XPS

ABSTRACT

This study addresses the high power impulse magnetron sputtering (HIPIMS) deposition of Ag-nanoparticle films on polyester and the comparison with films deposited by direct current pulsed magnetron sputtering (DCMSP). The first evidence is presented for the *Escherichia coli* bacterial inactivation by HIPIMS sputtered polyester compared to Ag–polyester sputtered by DCMSP. HIPIMS layers were significantly thinner than the DCMSP sputtered layers needing a much lower Ag-loading to inactivate *E. coli* within the same time scale. The Ag-nanoparticle films sputtered by DCMSP at 300 mA for 160 s was observed to inactivate completely *E. coli* within 2 h having a content of 0.205% Ag wt%/polyester wt%. HIPIMS-sputtered at 5 A for 75 s led to complete *E. coli* bacterial inactivation also within 2 h having a content Ag 0.031% Ag wt%/polyester wt%. The atomic rate of deposition with DCMSP is 6.2×10^{15} atoms Ag/cm^2 s while with HPIMS this rate was 2.7×10^{15} atoms Ag/cm^2 s. The degree of ionization of Ag^+/Ag^{2+} and Ar^+/Ar^{2+} was proportional to the target current applied during HIPIMS-sputtering as determined by mass spectroscopy. These experiments reveal significant differences at the higher end of the currents applied during HIPIMS sputtering as illustrated by the ion-flux composition. X-ray photoelectron spectroscopy (XPS) was used to determine the surface atomic concentration of O, Ag, and C on the Ag–polyester. These surface atomic concentrations were followed during the *E. coli* inactivation time providing the evidence for the *E. coli* oxidation on the Ag–polyester. X-ray diffraction shows Ag-metallic character for DCMSP sputtered samples for longer times compared to the Ag-clusters sputtered by HIPIMS leading to Ag-clusters aggregates. Ag-nanoparticle films on polyester sputtered by HIPIMS contain less Ag and are thinner compared to Ag-nanoparticle films sputtered by DCMSP.

1. Introduction

There is a growing concern about the increasing resistance to antibiotics of toxic bacteria like *Methycillin resistant staphylococcus aureus* (MRSA), *Acinetobacter* and *Pseudomonas aeruginosa* (*P. aeruginosa*) as well as *fungi* like Fusarium/*Candida Albicans* leading to hospital acquired infections (HAI) with the necessary high cost treatment and associated death of human beings having weak immune-system [1,2]. Ag-surfaces prepared by DCMS sputtering have been effective inactivating airborne bacteria [3]. Cu-surfaces prepared by DCMS [4] and DCMSP sputtering have recently been reported by our group [5]. DCMS-Ag deposition [6] has also been shown to be effective bacterial inactivation. These Ag-films present uniformity, acceptable bacterial inactivation kinetics, high adhesion and a relative low fabrication cost. These films on hospital textiles avoid the formation of bacterial biofilms that last for long times acting as a pump to spread toxic bacteria since they stick strongly to glass, prostheses and catheters [7–9].

High power impulse magnetron sputtering (HIPIMS) is gaining acceptance in many applications for surface treatments of metallic surfaces as a recent method for physical vapor deposition (PVD) based on magnetron sputtering [10]. The films deposited by HIPIMS protect metallic surfaces from corrosion and oxidation as well as wear and have revealed to be important in the deposition of metals on semiconductors and medical devices [10–12]. Recently Stranak et al. have reported HIPIMS for the deposition of Cu–Ti thin films [13,14,17,18]. Using HIPIMS, the high-density plasma at low pressures leads to a higher percentage of charged ions and a much higher metal-ion to neutral ratio as compared to DCMSP. The metal ion-to-neutral ratio for Ag in our case is estimated as 1:1 and much

* Corresponding author.
E-mail address: john.kiwi@epfl.ch (J. Kiwi).

1010-6030/$ – see front matter © 2011 Elsevier B.V. All rights reserved.
doi:10.1016/j.jphotochem.2011.10.017

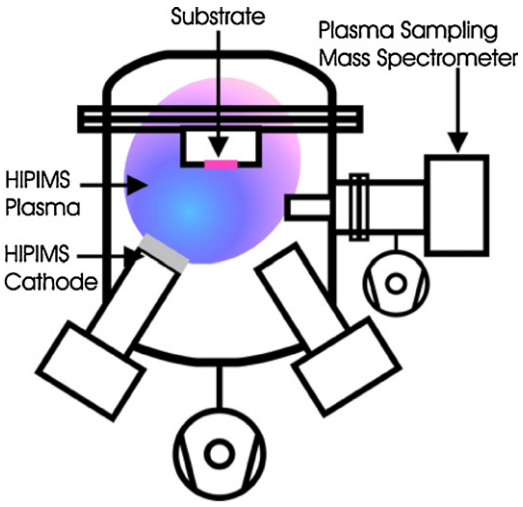

Fig. 1. Schematic of the HIPIMS setup, the cathode used was Ag and the substrate polyester.

higher compared to DCMSP with 1:9. In the case of HIPIMS a high plasma density close to the target ionizes effectively the sputtered metal-ions [11,12,24,26].

The objectives of this study are: (a) to present the first report of HIPIMS Ag-nanoparticle films at different HIPIMS-currents (A) and its effects on *Escherichia coli* kinetics inactivation, (b) to compare the inactivation kinetics of *E. coli* on Ag-nanoparticle films by DCMSP and HIPIMS, (c) to prepare antibacterial Ag-nanoparticle films avoiding the drawbacks of the wet techniques leading to non-uniform films on textiles [15,16,19,20] and finally (d) to report on the properties of Ag-nanoparticle films on polyester sputtered by DCMSP and HIPIMS.

2. Experimental

2.1. Ag-films on polyester, materials and Ag-nanoparticle film thickness calibration

HIPIMS deposition of Ag was carried out in a CMS-18 Vacuum system from Kurt Lesker Ltd. evacuated to 10^{-5} Pa by a turbomolecular pump [10]. Fig. 1 shows the schematic of the HIPIMS chamber. The Ag-cathode was 3 inches in diameter or 75 mm, Ag-99.99% from K. Lesker Ltd., UK. The HIPIMS was operated at 100 Hz with pulses of 100 ms separated by 10 ms. The HIPIMS current density at 5 A was 100 mA/cm^2. At a discharge voltage of 1700 V this corresponds to a power density of 170 W/cm^2. The HIPIMS short pulses avoid a glow-to-arc transition during plasma particle deposition [11]. The substrate was unbiased, and placed on an isolated holder, thus assuming the floating potential of the plasma. The substrate was not heated. The argon pressure was 0.4 Pa. The substrate-to-target distance was 15 cm. One Ag cathode was used. The polyester samples used were always 2×2 cm in size. The mass spectrometry measurements were carried out in a mass spectrometer PSM003 (Hiden Analytical Ltd.) to determine quantitatively the composition of the ions in the HIPIMS plasma Ar-atmosphere [27].

DCMSP sputtering on different textiles has been described recently laboratory [4–6]. DCMSP working pressure was 0.4 Pa, the distance between the Ag-target and the polyester fabric was 10 cm. DCMSP magnetron sputtering was operated at 50 kHz with 15% reversed voltage. A negative voltage was applied of −430 V and then the voltage was switched to +65 V (15% of −430 V). During DCMSP sputtering continuous pulses of 10 ms were applied, but with time the target gets overcharged and when this occurs. The unit tries three times to clear the charging arc additionally generating three

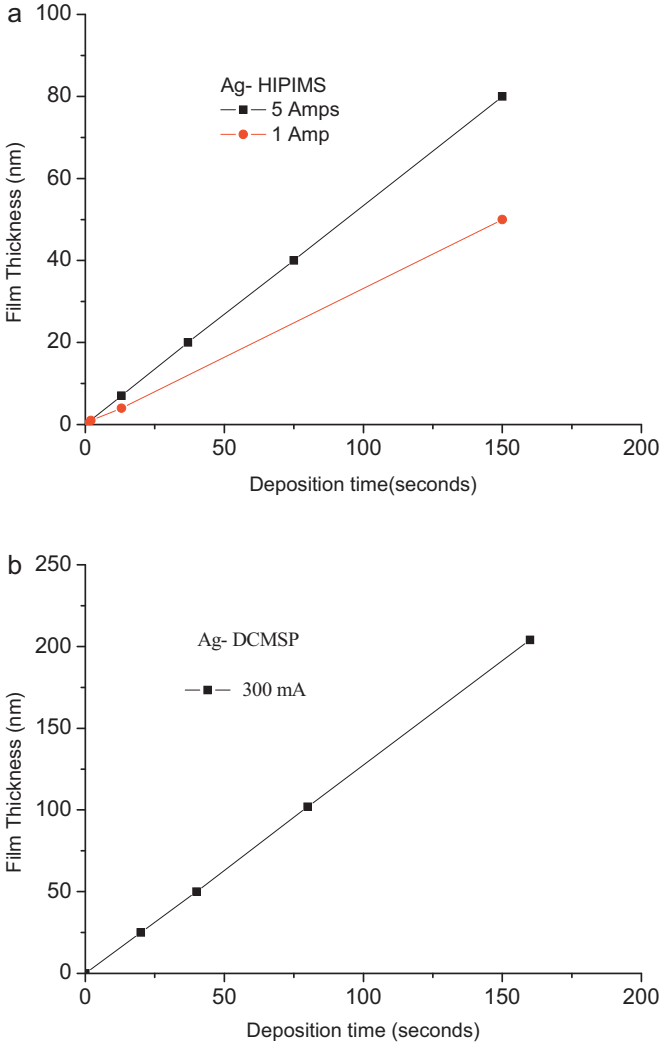

Fig. 2. (a) Calibration of the Ag-thickness by HIPIMS sputtered Si-wafers as a function of time for currents of 1 A and 5 A. (b) Calibration of the Ag-thickness deposited at 300 mA by DCMSP as a function of time on Si-wafers.

asymmetric pulses. The DCMSP at 300 mA on the 5 cm diameter DCMPS Ag-cathode provides a current density of 15.3 mA/cm^2.

The polyester used corresponds to the EMPA test cloth sample No. 407. It is a polyester Dacron polyethylene–terephthalate, type 54 spun, plain weave ISO 105-F04 used for color fastness determinations. The thermal stability of Dacron polyethylene–terephthalate was 110 °C for long-range operation and 140 °C for times ≤1 min. The thickness of the polyester was ±130 μm ±10%.

The calibration of the Ag-nanoparticle film thickness by HIPIMS and DCMSP on Si wafers is shown in Fig. 2. The film thickness was determined with a profilometer (Alphastep500, TENCOR). The nominal values of the thicknesses of the Ag-nanoparticle films on Si-wafers as well as the weight percentage of Ag on the polyester at different sputtering times using DCMSP and HIPIMS is shown in Table 1. The calibration traces in Fig. 2 for HIPIMS as well as for DCMSP presented an error of ±10%.

2.2. X-ray fluorescence determination of the Ag–polyester content

The Ag-content on the polyester was evaluated by X-ray fluorescence. By this technique, each element emits an X-ray of a

Table 1
Relation between the sputtering time used during DCMS, DCMSP and HIPIMS, the % Ag wt/wt and the film thickness.

	Time (s)	% Ag wt/wt	Thickness (nm)
DCMSP 300 mA			
	20	0.0259	25
	40	0.0430	50
	80	0.0870	102
	160	0.2050	204
HIPIMS 5 A			
	13	0.0029	7
	37	0.0086	20
	75	0.0315	40
	150	0.0630	80
HIPIMS			
1 A	2	0.002	2
1 A	13	0.003	4
2 A	3	0.014	7

certain wavelength associated with its particular atomic number. The spectrometer used was RFX, PANalytical PW2400.

2.3. Bacterial inactivation of E. coli on polyester samples covered by sputtered Ag film.

The samples of *Escherichia coli* (*E. coli* K12) was obtained from the Deutsche Sammlung von Mikroorganismen und Zellkulturen GmbH (DSMZ) ATCC23716, Braunschweig, Germany to test the antibacterial activity of the Ag–polyester fabrics. The polyester fabrics were sterilized by autoclaving at 121 °C for 2 h. 20 μL aliquot of culture with an initial concentration of 3.8×10^6 CFU mL^{-1} in NaCl/KCl (pH 7) was placed on each coated and uncoated (control) polyester fabric. The samples were placed on Petri dish provided with a lid to prevent evaporation. After each determination, the fabric was transferred into a sterile 2 mL Eppendorf tube containing 1 mL autoclaved NaCl/KCl saline solution. This solution was subsequently mixed thoroughly using a Vortex for 3 min. Serial dilutions were made in NaCl/KCl solution. A 100-μL sample of each dilution was pipetted onto a nutrient agar plate and then spread over the surface of the plate using standard plate method. Agar plates were incubated lid down, at 37 °C for 24 h before colonies were counted. The bacterial data reported were replicated three times and the media value of three experimental determinations is plotted in Figs. 4 and 5. To verify that no re-growth of *E. coli* occurs after the total inactivation observed in the first disinfection cycle, the Ag-nanoparticle film is incubated for 24 h at 37 °C. Then bacterial suspension of 100 μL is deposited on 3 Petri dishes to obtain the replica samples of the bacterial counting. These samples are incubated at 37 °C for 24 h. No bacterial re-growth was observed.

2.4. Composite transmission electron microscopy of Ag–polyester samples

A Philips CM-12 (field emission gun, 300 kV, 0.17 nm resolution) microscope at 120 kV was used to measure grain size of the Ag-film. The textiles were embedded in epoxy resin 45359 Fluka and the fabrics were cross-sectioned with an ultramicrotome (Ultracut E) and at a knife angle at 35°. Images were taken in Bright Field (BF) mode for the samples sputtered by DCMSP and HIPIMS.

2.5. X-ray diffraction measurements of Ag-nanoparticle film on polyester (XRD)

The identification of the Ag-nanoparticle peaks was carried out by means of an X'Pert diffractometer of the Philips, Delft, NL.

2.6. X-ray photoelectron spectroscopy of the Ag–polyester samples (XPS)

An AXIS NOVA photoelectron spectrometer (Kratos Analytical, Manchester, UK) equipped with monochromatic AlK$_\alpha$ ($h\nu$ = 1486.6 eV) anode was used during the study. The electrostatic charge effects on the samples were compensated by means of the low-energy electron source working in combination with a magnetic immersion lens. The carbon C1s line with position at 284.6 eV was used as a reference to correct the charging effect. The quantitative surface atomic concentration of some elements was determined from peak areas using sensitivity factors [20,21]. Spectrum background was subtracted according to Shirley [22]. The XPS spectra for the Ag-species were analyzed by means of spectra deconvolution software (CasaXPS-Vision 2, Kratos Analytical, UK).

3. Results and discussion

3.1. X-ray fluorescence of Ag–polyester sputtered samples

The HIPIMS unit is shown in Fig. 1. The Ag-content of the Ag-nanoparticle films for sputtered DCMSP and HIPIMS samples was determined by X-ray fluorescence. The most effective *E. coli* inactivation by a DCMSP sputtered sample during 160 s presented Ag-loadings of 0.205 Ag wt%/polyester wt%. This is ~6 times higher than the Ag wt%/polyester wt% found for HIPIMS samples sputtered for 75 s. The nominal thickness of the 160 s layer sputtered by DCMSP layer was 204 nm and the thickness observed for the HIPIMS sputtered layers for 75 s was 40 nm. This explains the lower content in Ag in the HIPIMS-sputtered sample compared to the DCMSP-sputtered sample. Both samples were of interest since they led to complete *E. coli* inactivation within a similar time of ~2 h as shown in Figs. 4 and 5.

3.2. Ag-films optical absorption as a function of sputtering time

Fig. 3 presents the Ag-nanoparticle films sputtered by HIPIMS for different times. The samples (a) polyester alone shows no color in the absence of Ag. A light brown grey-color appears in sample (b) shows dark-grey metallic Ag-color due to HIPIMS sputtered for 13 s at 5 A. The darker film on the polyester in Fig. 3c is due to the longer sputtering time of 75 s at 5 A.

The energy of Ag-ions is up to 30 eV and the average energy is 2 eV. In DCMS these energies are significantly lower with maximum of 2 eV and average of 0.1 eV. Although DCMSP energies can reach more than 100 eV due to the switch off of voltage at each pulse, this energy is delivered to the gas ions, which deliver it to the surface indirectly by bombarding the growing film. In HIPIMS the energy of the Ag-ions build up the Ag-film, thus delivering energy more efficiently to the growing Ag-particles on the surface. This results in denser films, with less porosity or voids. It also results in higher mobility on the surface and better ability to cover areas of the fiber that are out-of-sight of the plasma source. We are not set-up to measure the energy of the Ag-ions of the DCMSP sputtering so we cannot determine the exact values of the energy in the DCMSP experiments.

The Ag-atoms diffuse anisotropically on the textile surface and the subsequent migration/aggregation of the Ag-particle is driven by the high energy given to the Ag-ions leading to thermodynamically stable agglomerates [23,24]. But the high energy given to the Ag-ions can also be released when the Ag-ions arrive at the polyester surface recombining with surface electrons or bonding with the textile surface.

The color in Fig. 3 corresponds to the composite Ag/Ag_2O. The Ag_2O has been reported to have a band-gap (b_g) 0.7–1.0 eV vs

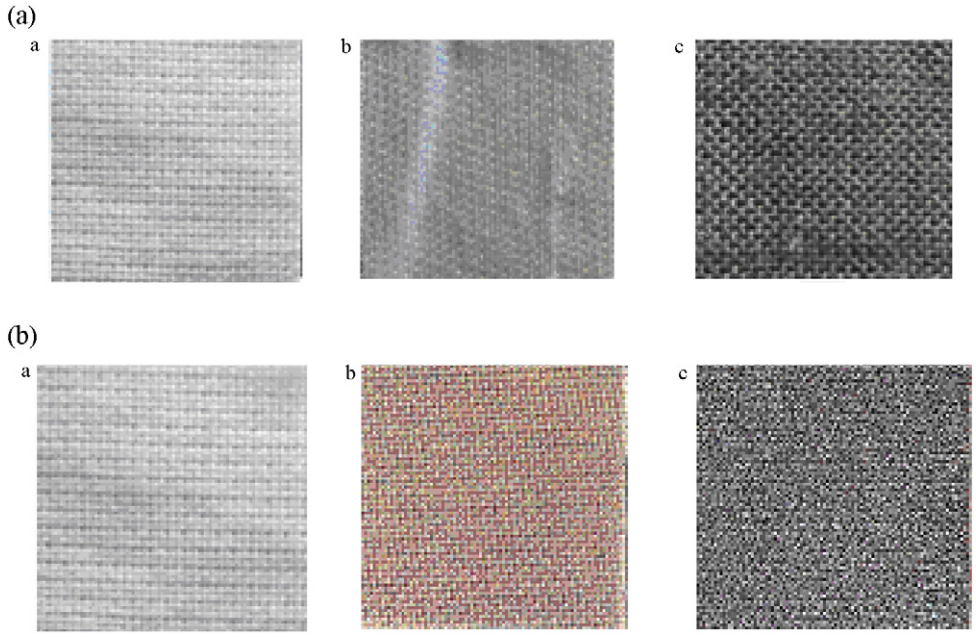

Fig. 3. (a) Polyester alone. (b) Ag-HIPIMS 13 s 5 A. (c) Ag-HIPIMS 75 s 5 A. (b) Samples: (a) polyester alone, (b) 20 s sputtered DCMSP 300 mA and (c) 160 s sputtered DCMSP 300 mA.

SCE and an absorption edge of 1000 nm [25]. Fig. 3a presents two Ag-nanoparticle films deposited by HIPIMS for 13 s coating of 7 Ag-layers with an Ag wt%/polyester wt% loading of 0.0029 as shown in Table 1. The HIPIMS sputtered sample for 75 s shows a darker color compared to the HIPIMS sputtered layers due to the thicker Ag-nanoparticle films of 40 nm with a loading of 0.0315 Ag wt%/polyester wt%, Fig. 3b) presents Ag-nanoparticle films sputtered by DCMSP at different times. We use the term Ag-nanoparticle films since the films are continuous and composed of nano-sized grains.

3.3. *E. coli* inactivation kinetics mediated DCMSP Ag-sputtered polyester

Fig. 4 presents the results of the *E. coli* inactivation by Ag-nanoparticle films DCMSP-sputtered at 300 mA. The most favorable *E. coli* inactivation kinetics within 2 h is seen in Fig. 4 for samples sputtered for 160 s. Taking 0.3 nm as the lattice distance of Ag-atoms, about 10^{15} atoms/cm^2 can be estimated for one atomic layer. Since one atomic layer is ~0.2 nm thick and Table 1 indicates that a thickness of 204 nm has been deposited in 160 s equivalent to 1020 layers then ~10^{18} atoms/cm^2 are necessary in Fig. 4 to induce the fastest *E. coli* degradation. The atomic rate of deposition with DCMSP was 6.2×10^{15} atoms Ag/cm^{2}s.

3.4. *E. coli* inactivation kinetics mediated by HIPIMS sputtered polyester

Fig. 5 presents the results for the *E. coli* inactivation by Ag-nanoparticle films sputtered at different times by HIPIMS 5 A. HIPIMS sputtering for 13 s lead to the threshold value for complete *E. coli* inactivation on an Ag-film 7 nm thick (Table 1). The threshold coating of 7 nm is equivalent to 35 layers with a content of 3.5×10^{16} atoms Ag/cm^2. The atomic rate of deposition with HIPIMS therefore is 2.7×10^{15} atoms Ag/cm^{2}s. DCMSP sputtering has been reported to proceed with a degree of ionization Ag between 3% and 10% with a plasma electron density much lower than the one taking place in the HIPIMS chamber [11,12,20,22]. This leads to different microstructures for the Ag-nanoparticle film on the polyester fabric.

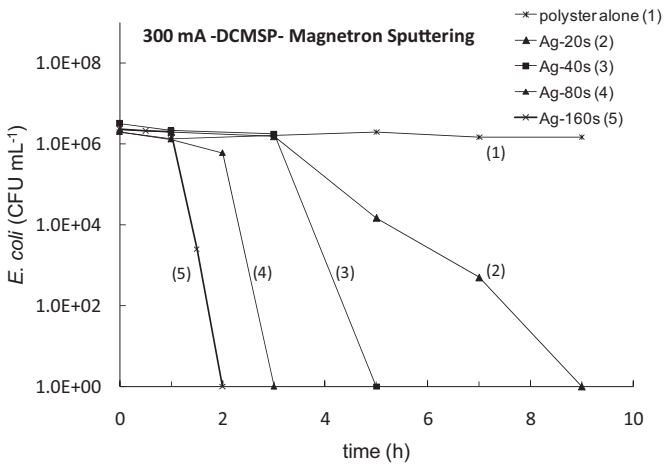

Fig. 4. *E. coli* inactivation kinetics as a function of time on Ag–polyester DCP-sputtered at different times applying currents of 300 mA.

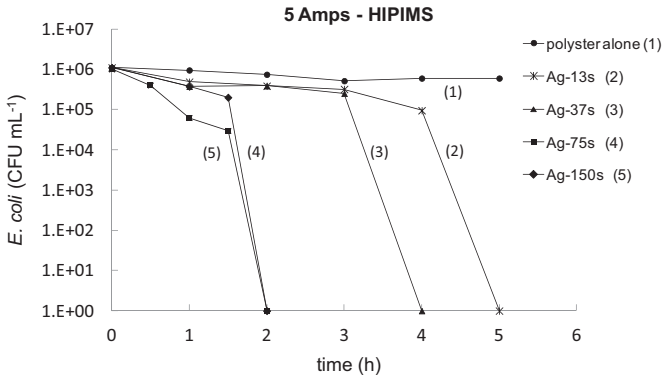

Fig. 5. *E. coli* inactivation kinetics as a function of time for HIPIMS sputtered Ag–polyester at 5 A.

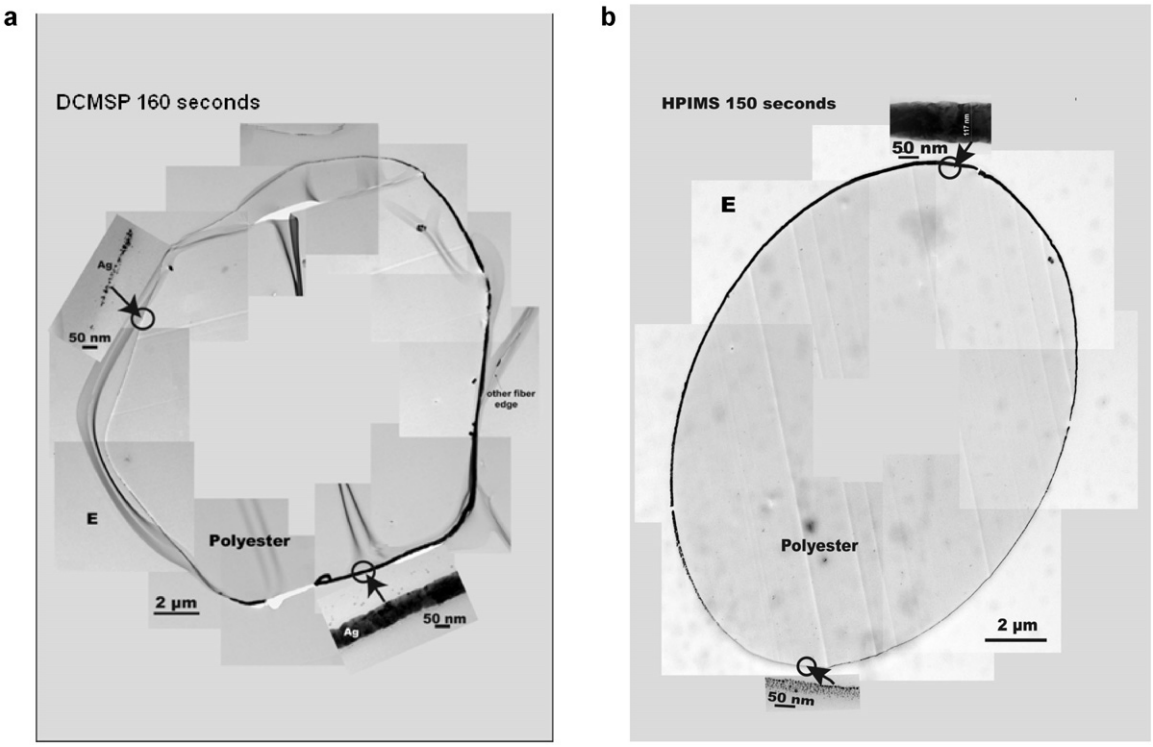

Fig. 6. (a) Transmission electron microscopy of polyester fiber DCMSP sputtered for 160 s at 300 mA. E in stands for epoxide used during the preparation of the samples for TEM analysis. (b) Transmission electron microscopy of Ag–polyester fibers sputtered by HIPIMS at 5 A for 150 s. E in stands for epoxide used during the preparation of the samples for TEM analysis.

3.5. Electron microscopy of Ag-polyester fibers determined by DCMSP and HIPIMS

Fig. 6a shows the composite TEM results for Ag-nanoparticle film on a full fiber sputtered by DCMSP for 160 s. The arrow on the lower side indicates the incident direction of the Ag-particles sputtered from the Ag-target in the magnetron chamber. A dark >100 nm thick is observed on the incident side along the axis of the Ag-target. But only a 5–15 nm thick Ag-nanoparticle film was found on the opposite side of the fiber in Fig. 6a. About 60–65% of the full polyester fiber was covered with Ag-nanoparticles. These nanoparticles are responsible for the transfer of electron/charges between the Ag-nanoparticle film and the *E. coli* in suspension.

Fig. 6b shows the HIPIMS sputtered Ag-nanoparticle film at 5 A during 150 s. The thick Ag-nanoparticle film 70–90 nm reaches up to 80–85% of the full fiber. At the bottom of the fiber only a thin layer of Ag was observed.

In the preceding paragraph the Ag-nanoparticle film deposited by DCMSP presented a larger thickness compared with thinner HIPIMS film layers as described in Table 1. Such a comparison is very problematic, since Ag-films with the same thicknesses should be compared. The size of the Ag-particles does not correlate with the Ag-film thickness as shown by Ag-layers obtained by EM and reported in Fig. 6a and b. By DCMSP sputtering particles 5–15 nm in size were observed when the Ag-nanoparticle film was about 100 nm thick, but also when the film showed a 5–15 nm thickness. In the case of HIPIMS the Ag-nanoparticle film, the thick coating on one side of the fiber and the thin coating on the opposite side of the fiber presented Ag-particles with about the same size (Fig. 6b).

The increased kinetic energy of the Ag-ions and ion-flux in the HIPIMS plasma is due to the increased current density of 100 mA/cm^2 vs 15.3 mA/cm^2 for DCMSP at 300 mA. The lower Ag-deposition of 0.0315 Ag wt%/polyester wt% obtained by HIPIMS compared to the DCMSP value of 0.2050 Ag wt%/polyester wt% leading to *E. coli* inactivation within 2 h can be attributed to the higher Ag-adatom mobility induced by HIPIMS. By HIPIMS the Ag-ions reach the polyester fiber from all directions in the plasma chamber [12,26] (see Fig. 1). HIPIMS is able to provide a much higher number of Ag neutrals and Ag-ions compared to DCMSP [10–12]. The ion-energies reach up to 30 eV as measured by energy-resolved mass spectroscopy measurements (not shown see Section 3.6). This is the intrinsic energy of ions in the plasma delivered by the sputter process and conserved at high level by excessive gas rarefaction caused by heating by the high instantaneous power on the target. Electron densities of $\sim 10^{18}$ (e^-/m^3) were estimated from the target current density.

In the magnetron sputtering chamber the ionization $Ar \rightarrow Ar^+ + e^-$ leads to a second step $e^- + Ag^\circ \rightarrow Ag^+ + 2e^-$. The high-speed electron collides with Ag° and kicks off a second electron leading to the Ag-ion. In the case of DCMSP, with a low content of Ag-ions the positive plasma is not strongly attracted to the negatively biased polyester fabric. But In the case of HIPIMS, the highly positive Ag-ions in the sputtering chamber are strongly attracted towards to the negative biased polyester making it possible to reach a much larger fraction of the full polyester surface compared to DCMSP-sputtering.

Ag-films on the polyester form by nucleation followed by growth, starting from Ag-atoms and leading to clusters. As the sputtering progresses these clusters grow, coalesce and finally lead to the Ag-nanoparticle film consisting of many layers. Nucleation seems to be the rate-determining step. The atomic layer(s) of the crystal(s) are a product of the nucleation process of the small clusters. The Ag-atoms diffuse anisotropically or isotropically on the polyester leading to the formation associating into bigger units. In our case, Ag metal/ions condense on the surface of the polyester binding to more Ag atoms. This leads to the production of Ag-clusters that become compact but not necessarily crystallographic [27–29].

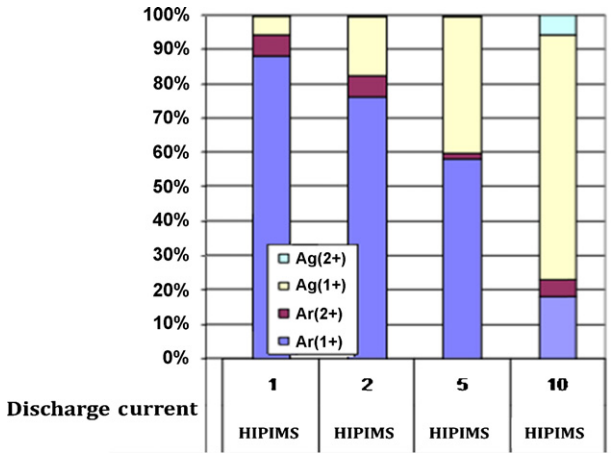

Fig. 7. Plasma ion-composition analysis of HIPIMS in Argon, derived from mass spectroscopy analysis. HIPIMS is applied at different currents as indicated in the figure.

3.6. Ion composition of plasma in sputtering obtained by mass spectroscopy

Fig. 7 presents the ion-composition when sputtering Ag by HIPIMS in an Ar atmosphere showing the mass spectroscopy analysis. The HIPIMS runs show that with increasing current the Ar^+-ions decreases and the Ag^+-ions in the gas phase increase. The amount of Ag-ions increased with peak HIPIMS discharge current. At discharge currents greater than 5 Amps, Ag^+-ions exceeded the amount of Ar^+-ions. The most interesting result is that HIPIMS discharges at 10 A peak current produced high quantities of Ag^+-ions with a small amount of Ag^{2+}-ions. In Fig. 7 when applying 10 A in the HIPIMS chamber, we observe the production of a small amount of Ag^{2+}-ions as shown by the data in the upper right corner of Fig. 7. In the current experiments HIPIMS power densities are at least a factor of 4–10 higher than more traditional sputtering methods such as DCMSP. Therefore, significant differences are expected between HIPIMS and DCMP-sputtering especially at the higher end as illustrated by the ion-flux composition in Fig. 7. The composition of HIPIMS at the lowest current of 1 A (current density of 20 mA/cm^2) was similar to the case of DCMSP sputtering with a current of 300 mA (current density of 15.3 mA/cm^2). In the presence of O_2 the Ag^{2+}-ion leads to AgO as reported recently [3].

3.7. X-ray diffraction of HIPIMS sputtered Ag–polyester (XRD)

Fig. 8 shows the XRD for Ag-nanoparticle films on polyester sputtered by DCMSP for 20 s and 160 s. The cluster formation occurs when Ag-atoms bind to other metal-atoms rather than to polyester. The growth of Ag-adatoms into clusters in the case of the 20 s sample leads to near spherical but not necessarily crystallographic Ag-clusters. At a longer sputtering time of 160 s, a steep peak is observed in Fig. 8 assigned to the Ag-metal peak at $\theta = 38^\circ$. Ag-metal nanoparticles have been reported with dimensions >1 nm [27]. HIPIMS sputtering for 13 s at 1 A indicate in the insert a low Ag-cluster formation. These clusters grow into bigger aggregates when sputtered for 75 s at 5 A, but did not lead to Ag-metal formation. More details describing the relation between the nano-crystallite particle size and lattice parameters of silver clusters have been recently reported [28,29]. We have not looked in a detailed way in Fig. 8 into the effect of the microstructure changes introduced in the Ag-nanoparticle HIPIMS sputtered for 75 s at 5 A leading to the formation of a thick 40 nm film compared to a thin 4 nm film sputtered for 13 s at 1 A.

Table 2
Atomic percentage surface concentration of Ag, O, C on HIPIMS sputtered polyester as a function of time during *E. coli* inactivation.

	Time	Element	% At. Conc.
HIPIMS 75 s 5 A			
	0 min	O 1s	14
		C 1s	52
		Ag 3d6	34
	30 min	O 1s	19
		C 1s	56
		Ag 3d6	25
	120 min	O 1s	25
		C 1s	72
		Ag 3d6	3

Table 3
Evolution of the C–C species and the oxidized species (C–OH, C–OC, carboxyl) on Ag–polyester sputtered for 75 s at 5 A with HIPIMS.

Time	Functionality	Peak position (eV)	Area	% At. Conc.
HIPIMS 75 s 5 A				
0 min	C–C	285.0	2902.5	61.7
	C–OH	286.1	786.4	16.7
	C–O–C	287.0	543.2	11.5
	Carboxyl	289.1	474.0	10.1
60 min	C–C	285.0	2211.1	56.8
	C–OH	286.3	772.1	19.8
	C–O–C	287.1	343.4	8.8
	Carboxyl	289.0	566.0	14.5
90 min	C–C	285.0	1690.6	38.5
	C–OH	286.8	911.2	20.8
	C–O–C	288.1	532.3	12.1
	Carboxyl	289.3	616.9	14.1

3.8. X-ray photoelectron spectroscopy of Ag–polyester samples within the E. coli inactivation time

Table 2 shows the atomic surface concentration of O, C and Ag for the HIPIMS sputtered sample for 75 s at 5 A. The increase of the surface O is due to the appearance C–OH, C–O–C and carboxyl species as the *E. coli* inactivation time progresses as shown in Table 2 due to bacterial oxidation [30,31]. At the same time, the C-content increases with reaction time and the Ag on the topmost 10 surface layers (<2 nm) is seen to decrease due to the C-residues left by the inactivated bacteria on the polyester surface.

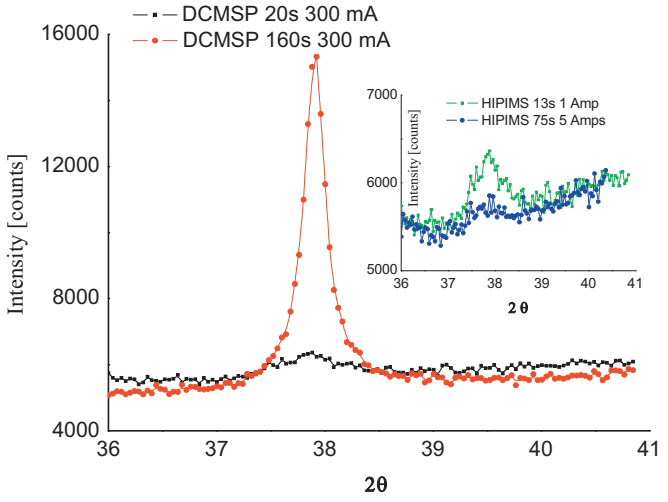

Fig. 8. X-ray diffraction of DCMS and HIPIMS sputtered Ag–polyester fibers sputtered under different conditions. For other details see text.

Table 3 shows the peaks area of the C–C species (including the reduced C-forms C=C, C–H) with (BE) of 285 eV and the deconvoluted oxidized C-forms of: C–OH, C–O–C and carboxyl functionalities with BE at 286.1 eV, 287.0 eV and 289.1 eV respectively [32]. The increase in the ratio C–OH + C–O–C + carboxyl/C–C was: 0.62 at zero time; 0.76 (at 60 min) and 1.48 (at 90 min) during the *E. coli* inactivation time [33]. The bacterial inactivation process induces a progressive decrease of the C–C species in the polyester (Table 3).

4. Conclusions

The results of our investigations have been summarized as follows:

- Low Ag content in the films sputtered by HIPIMS gives more effective *E. coli* inactivation compared to those sputtered by DCMSP. The material saving of non-renewable Ag is shown in this study.
- The most effective *E. coli* inactivation by DCMSP sputtered for 160 s had a loading of 0.2050% Ag/wt polyester ~7 times higher than the loading required by HIPIMS of 0.0315% Ag wt/wt polyester sputtered for 75 s.
- The HIPIMS deposited Ag-nanoparticle fibers present a different microstructure compared to DCMSP sputtering. This allows the bacterial inactivation to proceed in similar times compared to DCMPS-samples in spite of having a much lower loading of Ag/cm^2.
- The nominal thickness of the Ag-HIPIMS film of 40 nm was about 5 times lower than the Ag-film 204 nm thickness attained with DCMSP inducing a faster *E. coli* inactivation kinetics.
- The HIPIMS sputtered Ag-films show uniformity, effective bacterial inactivation performance and good adhesion.
- The Ag-films obtained by HIPIMS on the polyester show an increased metallic character as a function of sputtering time as shown by XRD.

Acknowledgements

We wish to thank the COST Action MP0804 Highly Ionized Pulse Plasma Processes (HIPIMS), the EPFL and the Swiss-Hungarian Cooperation program "Sustainable fine chemicals pharmaceutical industry: screening and utilization of liquid wastes" for the support of this work.

I have obtained permission of Dr Meech for this.

References

[1] A. Kramer, I. Schwebke, G. Kampf, How long do socomial pathogens persist in on inanimate surfaces? BMC Infect. Dis. 6 (2006) 130–138.
[2] S. Dancer, The role of the environmental cleaning in the control of hospital acquired infections, J. Hosp. Infect. 73 (2009) 378–385.
[3] I. Mejía, G. Restrepo, J. Marín, R. Sanjines, C. Pulgarín, E. Mielczarski, J. Mielczarski, J. Kiwi, Magnetron-sputtered Ag-modified cotton textiles active in the inactivation of airborne bacteria, ACS Appl. Mater. Interf. 2 (2010) 230–235.
[4] C. Castro, R. Sanjines, C. Pulgarin, P. Osorio-Vargas, A. Giraldo, J. Kiwi, Structure-reactivity relations of the Cu-cotton sputtered layers during *E. coli* inactivation in the dark and under light, J. Photochem. Photobiol. A 216 (2010) 295–302.
[5] P. Osorio-Vargas, R. Sanjines, C. Ruales, C. Castro, C. Pulgarin, A.-J. Rengifo-Herrera, J.-C. Lavanchy, J. Kiwi, Antimicrobial Cu-functionalized surfaces prepared by bipolar asymmetric DC-pulsed magnetron sputtering (PMS), J. Photochem. Photobiol. A 220 (2011) 70–76.
[6] O. Baghriche, A. Zertal, R. Sanjines, C. Ruales, C. Pulgarin, I. Stolitchnov, J. Kiwi, Ag-surfaces sputtered by DC and pulsed DC-magnetron sputtering effective in bacterial inactivation: testing and characterization, Surf. Coat. Technol., doi:10.1016/j.surfcoat.2011.10.041, in press.
[7] A.H. Foster, D.W. Sheel, P. Sheel, P. Evans, S. Varghese, N. Rutschke, H.M. Yates, Antimicrobial activity of titatnia/silver and titania/copper films prepared by CVD, J. Photochem. Photobiol. A. 216 (2010) 283–289.
[8] P.S.M. Dunlop, C.P. Sheeran, J.A. Byrne, M.A.S. McMahon, M.A. Boyle, K.G. McGuigan, Inactivation of clinically relevant pathogens by photocatalytic coatings, J. Photochem. Photobiol. A 216 (2010) 303–3010.
[9] E. Rupp, T. Fitzgerald, N. Marion, V. Helget, S. Puumala, R. Anderson, D. Fey, Effect of silver coated urinary catheters: efficacy, cost effectiveness and antimicrobial resistance, Am. J. Infect. Control 32 (2004) 445–452.
[10] A.P. Ehiasarian, A. Vetushka, A. Hecimovic, S. Konstantinidis, Ion composition produced by high power impulse magnetron sputtering discharges near the substrate, J. Appl. Phys. 104 (2008) 083305.
[11] A.P. Ehiasarian, R. New, W-D. Münz, L. Hultman, U. Helmersson, V. Kouznetsov, High power magnetron sputtered CrNx films, Vacuum 65 (2002) 147–154.
[12] K. Sarakinos, J. Alami, S. Konstantinidis, High power pulsed magnetron sputtering: a review on scientific and engineering state of the art, Surf. Coat. Technol. 204 (2010) 1661–1684.
[13] V. Stranak, M. Cada, Z. Hubicka, M. Tichy, R. Hippler, Time-resolved investigation of dual high power impulse magnetron-sputtering with closed magnetic field during deposition of Ti–Cu thin films, J. Appl. Phys. 108 (2010) 043305.
[14] V. Stranak, S. Drache, M. Cada, Z. Hubicka, M. Tichy, R. Hippler, Time-resolved diagnostics of dual high power impulse magnetron sputtering with pulse delays of 15 s and 500 s, Contrib. Plasma Phys. 51 (2011) 237–245.
[15] T. Yuranova, A.-G. Rincon, A. Bozzi, S. Parra, C. Pulgarin, P. Albers, J. Kiwi, Antibacterial textiles prepared by RF-plasma and vacuum-UV mediated deposition of silver, J Photochem. Photobiol. A Chem. 161 (2003) 27–34.
[16] T. Yuranova, A.-G. Rincon, C. Pulgarin, D. Laub, N. Xanthopoulos, H-J. Mathieu, J. Kiwi, Performance and characterization of Ag-cotton and Ag/TiO_2 loaded textiles during *E. coli* abatement, J. Photochem. Photobiol. A 181 (2006) 363–436.
[17] J. Musil, M. Louda, R. Cerstvy, P. Baroch, I.B. Ditta, A. Steele, H.A. Foster, Two-functional direct current sputtered silver-containing titanium dioxide thin films, Nanoscale Res. Lett. 4 (2009) 313–320.
[18] V. Ondok, J. Musil, M. Meissner, R. Cerstvy, K. Fajfrlik, Two-functional DC-sputtered Cu-containing TiO_2 thin films, J. Photochem. Photobiol. A 209 (2010) 158–162.
[19] A.P. Ehiasarian, Y.A. Gonzalvo, T.D. Whitmore, Plasma process time resolved studies of the high power impulse magnetron discharge in mixed Ar and N-atmosphere, Polymer 4 (2007) 5309–5313.
[20] D. Briggs, M. Shea, Practical Surface Analysis Auger and X-rays, vol. 1, 2nd ed., John Wiley & Sons, Chichester, New York, Toronto, Singapore, 1988.
[21] C.D. Wagner, M.W. Riggs, E.L. Davis, G.E. Mullenberg (Eds.), Handbook of X-ray Photoelectron spectroscopy, Perkin-Elmer Corporation Physical Electronics Division, Minnesota, 1979.
[22] A.D. Shirley, Corrections of electrostatic charged species in SP-spectroscopy, Phys. Rev. B5 (1972) 4709–4716.
[23] W.J. Mathews (Ed.), Epitaxial Growth. Part B. Nucleation of thin Films, Academic Press, New York, 1975, pp. 382–486, Chapter 4.
[24] J.P. Kelly, R.D. D.R. Arnell, Magnetron sputtering: a review of recent developments and applications, Vacuum 56 (2000) 159–172, and references therein.
[25] O.V. Krylov, Catalysis by Nonmetals, Academic Press, New York, 1980, p. 248.
[26] J. Lin, J. Moore, W. Sproul, B. Mishra, Z. Wu, Wang, The structure and properties of CrN coatings deposited using dc, pulsed dc and modulated pulse power magnetron sputtering, Surf. Coat. Technol. 204 (2010) 2230–2239.
[27] R. Houk, B. Jacobs, F. Gabaly, N. Chang, D. Graham, S. House, I. Roberstson, M. Allendorf, Silver Cluster Formation, Dynamics, and Chemistry in Metal-Organic Frameworks, Nano Letts. 9 (2009) 3413–3418.
[28] S. Turner, O. Lebedev, F. Schroeder, D. Esken, A. Fisher, V. Tendeloo, Direct imaging of loaded metal-organic framework materials, Chem. Mater. 20 (2008) 5622–5627.
[29] I. Shyjumon, M. Gopinadhan, O. Ivanova, M. Quaas, H. Wulff, C.A. Helm, R. Hippler, Structural deformation, melting point and lattice parameter studies of size selected silver clusters, Eur. Phys. J. D 37 (2006) 409–415.
[30] F. Mazille, T. Schoettl, C. Pulgarin, Synergistic effect of TiO_2 and iron oxide supported on fluorocarbon films. Part 1. Effect of preparation parameters on photocatalytic degradation of organic pollutant at neutral pH, Appl. Catal. B 89 (2009) 635–644.
[31] M. Dhananjeyan, E. Mielczarski, K. Thampi, Ph. Buffat, M. Bensimon, A. Kulik, J. Mielczarski, J. Kiwi, Photodynamics and surface characterization of immobilized TiO_2 and Fe_2O_3 photocatalysts modified polyethylene films, J. Phys. Chem. B 105 (2001) 12046–12055.
[32] O. Akhavan, E. Ghaderi, Photocatalytic reduction of graphene oxide nanosheets on TiO_2 thin film for photoinactivation of bacteria in solar light irradiation, J. Phys. Chem. C 113 (2009) 20214–20220.
[33] S. Yumitori, Correlation of C1s chemical state intensities with the O1s intensity in the XPS analysis of anodically oxidized glass-like carbon samples, J. Mater. Sci. 35 (2000) 139–146.